Rotational Spectra and Conformational Structures of 1-Phenyl-2-propanol, Methamphetamine, and 1-Phenyl-2-propanone

M. J. Tubergen*

Department of Chemistry, Kent State University, Kent, Ohio 44242

R. J. Lavrich,† D. F. Plusquellic, and R. D. Suenram

Optical Technology Division, National Institute of Standards and Technology, Gaithersburg, Maryland 20899-8441

Received: July 27, 2006; In Final Form: October 11, 2006

Microwave spectra have been recorded for 1-phenyl-2-propanol, methamphetamine, and 1-phenyl-2-propanone from 11 to 24 GHz using a Fourier-transform microwave spectrometer. Only one spectrum from a single conformational isomer was observed for each species. The rotational transitions in the spectrum of 1-phenyl-2-propanone were split into separate transitions arising from the A- and E-torsional levels of the methyl rotor. The fit of the E-state transitions to a "high-barrier" internal rotation Hamiltonian determines $V_3 = 238(1)$ cm^{-1} and rotor-axis angles of $\theta_a = 87.7(5)°$, $\theta_b = 50.0(5)°$, and $\theta_c = 40.0(5)°$. Ab initio optimizations (MP2/6-31G*) and single-point calculations (MP2/6-311++G**) were used to model the structures of 1-phenyl-2-propanol, methamphetamine, and 1-phenyl-2-propanone. The lowest energy conformations of these species were found to be stabilized by weak OH$-\pi$, NH$-\pi$, and CH$-\pi$ hydrogen-bonding interactions. Moments of inertia, derived from the model structures, were used to assign the spectra to the lowest energy conformation of each species. A series of MP2/6-31G* partial optimizations along the internal rotation pathway were used to estimate the barrier to methyl rotation to be 355 cm^{-1} for 1-phenyl-2-propanone.

Introduction

Methamphetamine is a well-known synthetic stimulant (Figure 1B); because of the potency of its pharmacological effect, illegal methamphetamine production has become a serious criminal justice problem in many areas. Methamphetamine stimulates the release of dopamine, adrenaline, and serotonin and blocks their re-uptake by the central nervous system.[1,2]

Methamphetamine binds to the D1 and D2 receptors,[2] which are part of the 7TM superfamily of receptors.[3] While the structures of 7TM receptor proteins within membrane environments are not fully known, it is thought that there are seven α-helical regions which are embedded in the membrane. The binding of neurotransmitters and other ligands such as methamphetamine is thought to occur through hydrogen bonding to serine and aspartic acid residues in one of the transmembrane helices. Some, as yet unknown, change in receptor protein conformation is stimulated by ligand binding, and this change initiates the signal transduction into neural cells.[3]

A thorough understanding of the conformational structures of methamphetamine and their relative energies may add additional insight into the nature of its binding to the receptors as well as the energy changes that drive the binding. Conformational analysis of methamphetamine has previously been conducted at the HF/3-21G level as part of an investigation of the molecular origin of the increased biological activity of methamphetamine over that of amphetamine.[4] Sull et al. proposed that the additional methyl group in methamphetamine stabilizes the configuration best suited for receptor binding.[4] Takahashi et al. investigated the conformations of structurally related compounds 1-phenyl-2-propanol[5] (Figure 1A) and 1-phenyl-2-propanone (Figure 1C)[6] at the MP2/6-311G(d,p)//MP2/6-31G(d) level and found that intramolecular OH$-\pi$ and

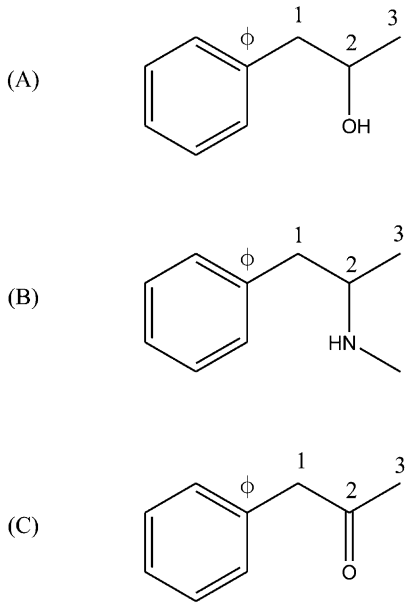

Figure 1. Molecular structures of (A) 1-phenyl-2-propanol, (B) methamphetamine, and (C) 1-phenyl-2-propanone.

* To whom correspondence should be addressed. E-mail: mtuberge@kent.edu.

† Current address: Air Pollution Prevention and Control Division, National Risk Management Research Laboratory, United States Environmental Protection Agency, E343-02 USEPA Mailroom, Research Triangle, NC 27711.

10.1021/jp064810u CCC: $33.50
Published on Web 11/21/2006

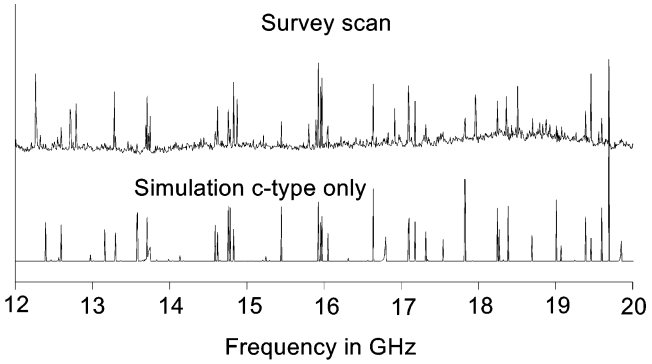

Figure 2. Survey scan of methamphetamine from 12 to 20 GHz.

CH$-\pi$ hydrogen-bonding interactions contribute to the stability of the lowest energy conformations.

There have been no experimental investigations of the conformations of 1-phenyl-2-propanol, methamphetamine, and 1-phenyl-2-propanone (parts A−C, respectively, of Figure 1). The high spectral resolution of Fourier-transform microwave spectroscopy can distinguish rotational spectra arising from different conformational structures of a given species, and the high sensitivity of the technique has been used to detect spectra arising from higher energy conformations in addition to the lowest energy structure.[7,8]

Finally, tunneling splittings from methyl group internal rotation can often be resolved,[9,10] providing quantitative data about the barrier height to internal rotation. The torsional barrier, in turn, may provide a measure of the strength of CH$-\pi$ hydrogen bonds in the case of 1-phenyl-2-propanone.

Experimental Method

Rotational spectra of methamphetamine (*N*-methyl-1-phenyl-2-propanamine), ^{15}N-methamphetamine, 1-phenyl-2-propanone, and 1-phenyl-2-propanol were recorded in the 11−24 GHz range using one of the mini Fourier-transform microwave (FTMW) spectrometers at NIST.[11] Survey scans were recorded by averaging the free induction decays for 10−50 nozzle pulses followed by Fourier transformation; the frequency step size for these scans was 500 kHz. A survey scan of methamphetamine in the range 12−20 GHz is shown in Figure 2.

The molecular beam was produced by a 1.2 mm diameter pulsed valve (General Valve series 9)[12] fitted with a reservoir nozzle.[13] Samples were individually placed in the heated reservoir nozzle mounted behind one of the mirrors of the resonant cavity, which also serves as a vacuum chamber flange. This arrangement provides for coaxial injection of the molecular beam and yields typical line widths of 10−20 kHz for the spectrometer that was used in this work.[11] Under these conditions, the type B (coverage factor $k = 1$ or 1σ) uncertainty on the frequency measurements is ±4 kHz.[14] 1-Phenyl-2-propanol was heated to 90 °C, methamphetamine was heated to 120 °C, and 1-phenyl-2-propanone was heated to 60 °C. Sample vapor was entrained in a helium/neon carrier gas mixture (20%/80% by volume) with a backing pressure of 200 kPa for expansion into the cavity. The rotational temperature in the expansion under these conditions is typically ∼2 K.

1-Phenyl-2-propanol was used as purchased from Aldrich. 1-Phenyl-2-propanone was prepared from 1-phenyl-2-propanol by oxidation with sodium dichromate in the presence of H_2SO_4. Methamphetamine was prepared from 1-phenyl-2-propanol by reductive amination with sodium cyanoborohydride and an excess of methylamine hydrochloride in methanol; ^{15}N-methamphetamine was prepared using ^{15}N-methylamine hydrochloride (Cambridge Isotope Laboratories).[12]

TABLE 1: Spectroscopic Constants of 1-Phenyl-2-propanol

rotational parameter	value	rotational parameter	value
A/MHz	3185.48214(2)[a]	δ_J/kHz	−0.0004(1)
B/MHz	752.074283(9)	δ_K/kHz	0.57(3)
C/MHz	687.844758(9)	σ/MHz	1.8
Δ_J/kHz	0.06601(2)	no. of transitions in the fit	59
Δ_{JK}/kHz	0.3715(3)		
Δ_K/kHz	0.3973(18)		

[a] The numbers shown in parentheses are type A uncertainties with $k = 1$ coverage or 1σ (ref 14).

Computational Method

Model structures for 1-phenyl-2-propanol, methamphetamine, and 1-phenyl-2-propanone were generated from ab initio calculations using the Gaussian03 suite of programs[15] on the Itanium-2 cluster at the Ohio Supercomputer Center. Optimizations were conducted at the MP2 level with the 6-31G* basis set; vibrational frequencies were calculated to distinguish conformational minima on the potential energy surface from saddle points, as well as to calculate the zero-point energy correction. Single-point calculations at the MP2/6-311++G** level were performed on the optimized geometries to obtain more precise conformational energies; the single-point energies were corrected for zero-point energies using the MP2/6-31G* frequency results.

Gauche and anti configurations of the side chains were used as starting structures for the optimizations. Nine unique structures with gauche and/or anti configurations can be formed by torsions about the C_1-C_2 and C_2-O bonds of 1-phenyl-2-propanol. Eighteen unique structures are possible for methamphetamine because of torsions about the C_1-C_2 and C_2-N bonds as well as the exchange of configuration at the amino nitrogen. Because of the planarity of the carbonyl group in 1-phenyl-2-propanone, only two unique orientations of the methyl group are possible about the C_1-C_2 bond.

Results and Discussion

1-Phenyl-2-propanol. Fifty-nine rotational transitions were measured for 1-phenyl-2-propanol in the 11.5−21.0 GHz frequency range. All three dipole selection rules were observed including 25 *a*-, 20 *b*-, and 14 *c*-type rotational transitions; the assigned transition frequencies of 1-phenyl-2-propanol are listed in Supporting Information Table 1. Rotational constants and quartic centrifugal distortion constants of the Watson asymmetric rotor Hamiltonian (I^r representation)[16] were fit to the transition frequencies using Pickett's SPFIT routine[17] in the CALPGM suite of programs,[18] and these constants are given in Table 1. No unassigned transitions that could be assigned to a second conformation or separate A- and E-torsional states were observed in the spectrum.

Nine gauche conformers of (*S*)-1-phenyl-2-propanol were optimized at the MP2/6-31G* level. These conformations are described by approximate values for the torsional angles $\tau_1 = C_\varphi-C_1-C_2-O$ and $\tau_2 = C_1-C_2-O-H$ (g, +60°; g′, −60°; a, 180°). These two torsion angles determine the positions of the hydroxyl and methyl groups as well as the orientation of the hydroxyl hydrogen. The relative energies of the MP2/6-31G*-optimized geometries and the corresponding MP2/6-311++G** single-point results, corrected for zero-point energies, are listed for each (*S*)-1-phenyl-2-propanol conformer in Table 2. Cal-

TABLE 2: Relative Energies and Dipole Moment Projections of (*S*)-1-Phenyl-2-propanol Conformers

conformer	ΔE^a/ kJ mol^{-1}	ΔE^b/ kJ mol^{-1}	μ_a/ D	μ_b/ D	μ_c/ D	ΔI_{rms}/ u Å^2
gg′	0.0	0.0	−1.36	1.26	0.25	6.6
g′g	2.0	3.4	1.30	1.40	0.14	90.8
g′a	7.1	5.3	1.22	−1.07	−0.82	82.4
aa	7.6	4.2	0.35	0.34	1.68	9.2
ag′	7.7	4.2	1.39	−1.07	−0.26	11.3
ga	7.9	7.2	−1.31	−0.85	−1.04	15.6
ag	8.1	5.6	1.10	1.39	−0.30	11.1
g′g′	9.1	8.1	−0.46	−0.64	−1.51	77.2
gg	10.8	10.9	−0.95	−0.77	1.40	15.9

[a] Relative to the gg′ conformer; MP2/6-31G*, includes zero-point energies. [b] Relative to the gg′ conformer; MP2/6-311++G**, includes zero-point energies (MP2/6-31G*).

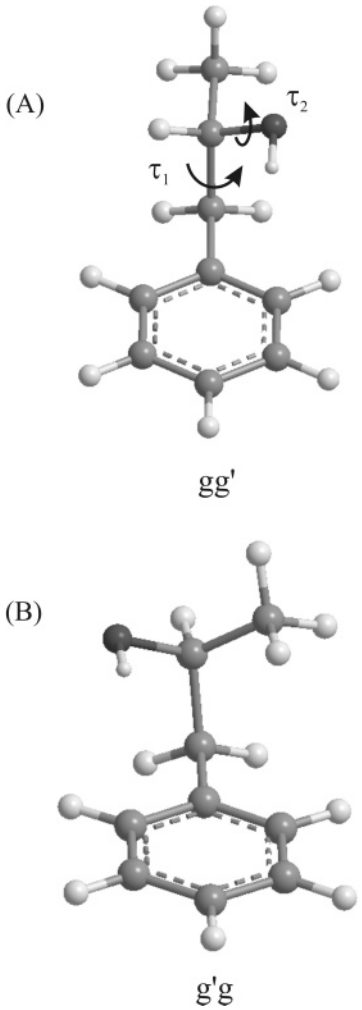

Figure 3. Structures of the (A) gg′ and (B) g′g conformers of 1-phenyl-2-propanol.

culated principal-axis projections of the molecular dipole moment and root-mean-square average differences between predicted and measured moments of inertia are also listed for each conformer in Table 2.

The gg′ conformer of 1-phenyl-2-propanol (Figure 3A) was found to be the single lowest energy structure at both the MP2/6-31G* and MP2/6-311++G** levels, while the remaining eight conformers were 2.0 kJ mol^{-1} or more above the gg′ minimum. For comparison with experiment, root-mean-square averages of the differences between the experimental moments of inertia and those calculated from the ab initio structures were calculated and are given as ΔI_{rms}, where $\Delta I = I_x(\text{exptl}) - I_x(\text{calcd})$ ($x = a$, b, and c). As can be seen from Table 2, the gg′ structure reproduces the phenylpropanol moments of inertia best. $\Delta I_{rms} = 6.6$ u Å^2 for gg′, but $\Delta I_{rms} > 9$ u Å^2 for the other eight structures. The dipole moment projections predicted for gg′ are also consistent with the observation of transitions with all three dipole selection rules.

TABLE 3: Spectroscopic Constants of ^{14}N-Methamphetamine and ^{15}N-Methamphetamine

rotational parameter	^{14}N-methamphetamine	^{15}N-methamphetamine
A/MHz	2121.7105(8)[a]	2113.2138(12)
B/MHz	613.2421(2)	610.7054(3)
C/MHz	575.5215(2)	572.6969(4)
Δ_J/kHz	0.0707(7)	0.0703(11)
Δ_{JK}/kHz	0.096(8)	0.125(14)
Δ_K/kHz	0.35(5)	0.37(8)
δ_J/kHz	0.0022(2)	0.0007(8)
δ_K/kHz	0.23(4)	0.27(9)
χ_{aa}/MHz	1.076(21)	
χ_{bb}/MHz	2.626(11)	
χ_{cc}/MHz	−3.701(13)	
σ/kHz	3.8	1.4
no. of transitions in the fit	31	15

[a] The numbers shown in parentheses are type A uncertainties with $k = 1$ coverage or 1σ (ref 14).

The ab initio optimizations of 1-phenyl-2-propanol reproduce the conformer energy ordering observed by Takahashi et al.[5] In particular, we observe that the two lowest energy conformers, gg′ and g′g (Figure 3B), orient the hydroxyl group toward the π-electrons, forming a weak intramolecular hydrogen bond. The OH$-\pi$ hydrogen bond is directed toward the phenyl ring above the midpoint of the $C_\varphi - C_{ortho}$ bond, and this interatomic distance has been used to characterize the OH$-\pi$ intramolecular hydrogen bond. This hydrogen bond distance is 2.406 Å for the gg′ conformer and 2.455 Å for the g′g conformer. While these hydrogen bond distances are somewhat (25%) longer than those found for strong hydrogen bonds from OH, they fall within the range of weak hydrogen bonds observed in the crystal structures of biological molecules.[19]

Methamphetamine. Thirty-one rotational transitions of the normal species of methamphetamine were measured in the 10.5−18.5 GHz frequency range shown in Figure 2. Because of the $I = 1$ nitrogen nucleus, nuclear quadrupole hyperfine interactions split the 10 *a*-type and 21 *c*-type rotational transitions into 88 hyperfine components. The assigned transitions of methamphetamine are listed in Supporting Information Table 2. The nuclear quadrupole coupling constants, rotational constants, and quartic centrifugal distortion constants of the Watson asymmetric rotor Hamiltonian (I^r representation)[16] were simultaneously fit to the transition frequencies using SPFIT,[17] and these constants are given in Table 3. This fit indicates that most of the observed transitions can be assigned to a rotational spectrum arising from a single conformational isomer of methamphetamine. Up to 10 more transitions were measured but could not be assigned to separate A- and E-torsional states or a spectrum of a second conformer. It is believed that these additional transitions arise from impurities or decomposition products.

Fifteen rotational transitions were measured for the ^{15}N-labeled methamphetamine; these transitions are listed in Supporting Information Table 3. Rotational constants and the quartic centrifugal distortion constants were fit to the transition frequencies using SPFIT,[17] and these constants are given in Table 3. The spectrum of ^{15}N-methamphetamine was contaminated by

TABLE 4: Relative Energies and Dipole Moment Projections of Methamphetamine Conformers

conformer	ΔE^a/ kJ mol^{-1}	ΔE^b/ kJ mol^{-1}	μ_a/ D	μ_b/ D	μ_c/ D	ΔI_{rms}/ u Å^2
gag′	0.0	0.0	−0.44	−0.12	−0.95	5.5
g′ag	2.8	5.4	0.23	0.50	−0.84	51.9
g′g′g	3.1	3.4	−0.70	−0.26	0.72	95.4
ag′a	5.1	4.2	0.20	−0.47	0.99	72.0
g′g′a	5.1	5.4	−1.47	0.45	0.10	58.9
aag′	5.9	5.2	0.07	−1.02	−0.35	118.0
ag′g	6.3	7.1	−0.33	−0.25	−0.92	73.6
aag	6.5	7.4	−0.25	−0.79	0.70	117.3
gg′a	7.6	4.6	0.98	0.05	−0.85	75.9
ggg′	7.7	7.1	−0.67	0.03	0.79	38.7
gag	8.0	10.8	1.60	−0.24	−0.2	26.9
g′ag′	8.2	9.3	1.27	−0.43	−0.53	26.4
gg′g	11.1	8.3	−1.13	−0.40	0.4	76.4
agg′	12.4	12.6	−0.39	−0.03	−0.96	88.6
aga	12.5	12.7	0.29	0.78	0.74	87.7
gga	14.6	15.1	1.58	−0.29	−0.27	38.8
g′ga	18.5	15.8	−0.97	−0.33	−0.67	139.2
g′gg′	21.7	17.8	1.05	−0.20	0.27	137.7

[a] Relative to the gag′ conformer; MP2/6-31G*, includes zero-point energies. [b] Relative to the gag′ conformer; MP2/6-311++G**, includes zero-point energies (MP2/6-31G*).

13 unassigned transitions. These unassigned transitions were often close to the transition frequencies of the dominant conformer of ^{15}N-methamphetamine, but they could not be assigned to separate A- and E-torsional states or to a second methamphetamine conformer. Instead it is likely that the unassigned transitions in the ^{15}N-methamphetamine spectrum arise from contaminants in the impure sample used for spectroscopy.

The 18 unique conformers found by optimization of gauche methamphetamine structures are listed in Table 4. These structures can be described by approximate values for the torsional angles $\tau_1 = C_\varphi - C_1 - C_2 - N$, $\tau_2 = C_1 - C_2 - N - C$, and $\tau_3 = C_1 - C_2 - N - H$ (g, +60°; g′, − 60°; a, 180°). The relative energies and calculated projections of the dipole moment onto the principal inertial axes of the molecule are listed for each conformer in Table 4; the relative energies are corrected for zero-point energies. The theoretical-versus-experimental root-mean-square differences in the moments of inertia for the two isotopic species are also given in Table 4. Finally, relative energies from the single-point calculations at the MP2/6-311++G** level are also given in Table 4.

The gag′ conformer (Figure 4A; $\tau_1 = 61°$, $\tau_2 = -169°$, $\tau_3 = -51°$) was found to have the lowest energy with both the 6-31G* and 6-311++G** basis sets. The structure of this conformer predicts moments of inertia that agree best with the experimental moments of inertia of both ^{14}N- and ^{15}N-methamphetamine; $\Delta I_{rms} = 5.5$ u Å^2 for the gag′ conformer. The model structure also correctly predicts the strong *c*-type and weaker *a*-type transitions that were experimentally observed.

The gag′ conformer of methamphetamine is stabilized by an NH−π hydrogen bond similar to the OH−π intramolecular hydrogen bond observed in the gg′ structure of 1-phenyl-2-propanol. The hydrogen bond distance to the midpoint of the $C_\varphi - C_{ortho}$ bond is 2.417 Å in this conformer of methamphetamine. The next two lowest energy conformers at the MP/6-31G* level, g′ag and g′g′g (Figure 4B,C), may also be stabilized by NH−π hydrogen bonds; the hydrogen bond lengths in these structures are 2.556 and 2.598 Å, respectively. The g′ag and g′g′g structures are about 3 kJ mol^{-1} higher in energy than the gag′ structure because the C_3 methyl group is gauche to the phenyl ring. The remaining conformer structures are calculated

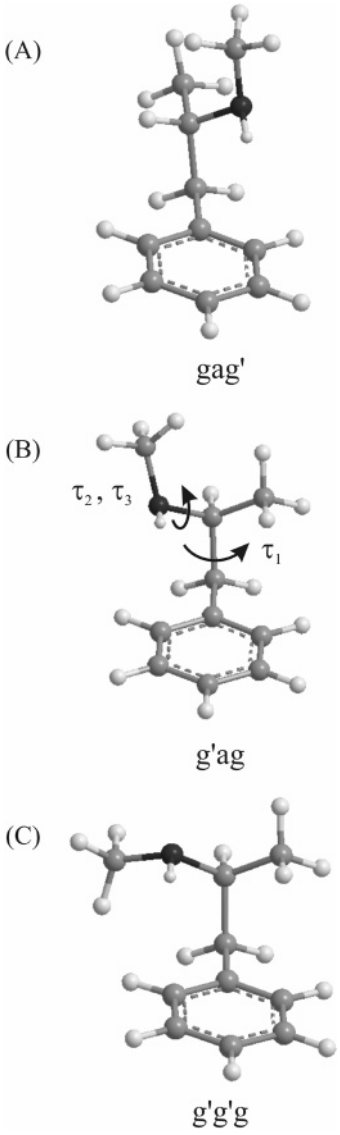

Figure 4. Structures of the (A) gag′, (B) g′ag, and (C) g′g′g′ conformers of methamphetamine.

to be much higher in energy, and all 17 higher energy conformers have moments of inertia that differ substantially from the observed values.

The larger basis set (6-311++G**) increases the relative energy of the g′ag conformer and partially changes the energy ordering of the higher energy conformers. The energy ordering of methamphetamine conformers was also found to be somewhat different from the ordering recently calculated at the HF/3-21G level. The calculations of Sull et al.[4] identify the g$^-$g$^-$a (using Sull's notation) conformation of protonated (*R*)-methamphetamine to be the lowest energy conformer; this structure is comparable to the optimized gag′ structure of (*S*)-methamphetamine. The energy ordering of the higher energy methamphetamine conformers in ref 4 differs significantly from that of Table 4 due to the effect of protonation and the small basis set that was used.

1-Phenyl-2-propanone. The rotational spectrum of 1-phenyl-2-propanone was measured from 12 to 25 GHz. Unlike the spectra of 1-phenyl-2-propanol and methamphetamine, the spectrum of 1-phenyl-2-propanone contained additional splittings from the A- and E-torsional levels of the methyl top. The A-state was assigned using the JB95 spectral fitting program[20] and fit to a Watson asymmetric rotor Hamiltonian (I^r representa-

TABLE 5: Rotational Parameters for the A- and E-States of 1-Phenyl-2-propanone

rotational parameter	A-state	E-state[c]
A/MHz	2855.4487(5)[b]	2855.3093(4)
B/MHz	832.9527(3)	832.9159(3)
C/MHz	748.9478(2)	748.8596(2)
Δ_J/kHz	0.161(2)	0.160(1)
Δ_{JK}/kHz	1.268(7)	1.245(7)
Δ_K/kHz	1.17(2)	1.23(2)
δ_J/kHz	0.0313(6)	0.0320(6)
δ_K/kHz	0.85(7)	0.82(7)
D_a/MHz		−2.341(1)
D_b/MHz		11.26(2)
D_c/MHz		12.006(4)
$G_{aaa}{}^a$/kHz		−5.3(37)[d]
$G_{aac}{}^a$/kHz		−8.7(13)[d]
$G_{cca}{}^a$/kHz		−3.1(2)[d]
V_3/cm^{-1}		238.(1)
F (fixed)		5.301
θ_a/deg		87.7(5)[e]
θ_b/deg		50.0(5)[e]
θ_c/deg		40.0(5)[e]
σ/kHz	3	2
no. of transitions in the fit	50	58

[a] The operators which these parameters multiply are $G_{aaa}\mathbf{P}_a{}^3$, $G_{aab}(\mathbf{P}_a{}^2\mathbf{P}_b + \mathbf{P}_a\mathbf{P}_b\mathbf{P}_a + \mathbf{P}_b\mathbf{P}_a{}^2)$, etc. [b] The numbers shown in parentheses are type A uncertainties with $k = 1$ coverage or 1σ (ref 14). [c] The rotational parameters for the E-state are given in the principal-axis frame. [d] These cubic terms are only marginally determined, but by including them in the fit, the observed − calculated values are all within the expected type B ($\sigma = 2$) experimental uncertainty of ±8 kHz (ref 14). [e] Angle of the methyl top with respect to the corresponding (subscripted) principal axis.

tion).[16] The active selection rules for the A-state were predominately *b*-type, with weaker *a*-type transitions also being observed. The 50 transitions used in the fit are listed in Supporting Information Table 4, and the resulting rotational parameters are given in Table 5.

The A-state transitions were accompanied by a second set of lines that were typically within 1 MHz of their positions and therefore were identified as belonging to the E-torsional state of the methyl rotor. It was straightforward to assign the E-state spectrum since the displacements from the corresponding A-state lines were not so large as to obscure the overall patterns. As described elsewhere,[9] the E-state parameters of the "high-barrier" Hamiltonian were fit to 58 transitions in the principal-axis frame. The three (linear operator) terms D_a, D_b, and D_c plus two (higher order) cubic terms in the torsion−rotation coupling were necessary to obtain spectral predictions commensurate with the quality of the A-state fit. In addition to transitions obeying *a*- and *b*-type selection rules, a few *c*-type transitions were located as a result of quantum-state mixing caused by these additional operators.

The E-state transition frequencies are listed in Supporting Information Table 5, and the rotational parameters from the fit are given in Table 5. Notice that, of the three linear terms, the D_a term is the smallest in magnitude, indicating the methyl rotor axis is nearly perpendicular to the *a*-inertial axis. Using a separate program,[9] the torsional barrier and rotor axis angles relative to the principal-axis frame were obtained from the A- and E-state parameters and are given in Table 5. Indeed, the angles place the rotor axis within 3° of the *b*,*c*-inertial plane. Furthermore, it is interesting that the torsional barrier of 238(1) cm^{-1} is roughly 3-fold larger than barriers reported for methyl rotors attached to the C-terminus of peptide bonds.[9,21,22] Even more surprising is the complete absence of resolvable splittings

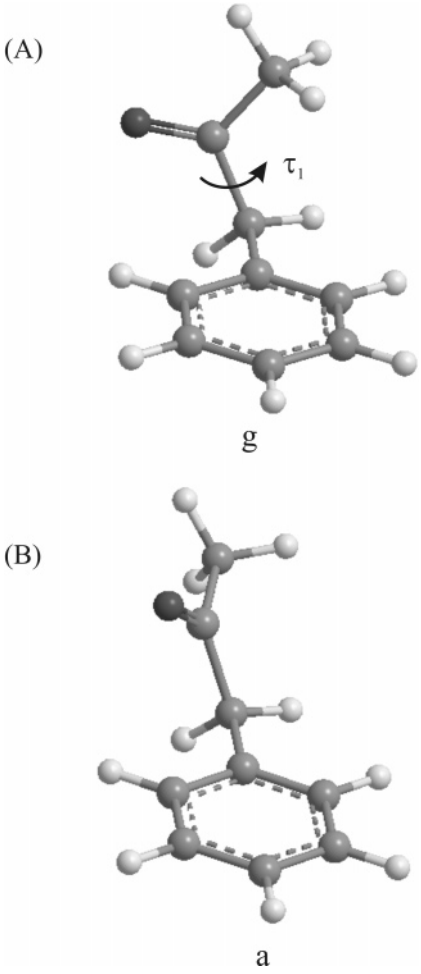

Figure 5. Structures of the (A) gauche and (B) anti conformers of 1-phenyl-2-propanone.

TABLE 6: Relative Energies and Dipole Moment Projections of 1-Phenyl-2-propanone Conformers

conformer	ΔE^a/ kJ mol^{-1}	ΔE^b/ kJ mol^{-1}	μ_a/ D	μ_b/ D	μ_c/ D	ΔI_{rms}/ u Å^2
gauche	0.0	0.0	1.62	−2.71	0	9.9
anti	4.5	6.1	0.88	2.31	1.72	44.3

[a] Relative to the g conformer; MP2/6-31G*, includes zero-point energies. [b] Relative to the g conformer; MP2/6-311++G**; includes zero-point energies (MP2/6-31G*).

from the amide methyl (N-terminus) rotor of methamphetamine. Perhaps the reason for these differences can be understood in terms of the nonplanarity of these fragments relative to those of the peptide bond.

To explore these structural issues, ab initio calculations were performed on the two unique conformers of 1-phenyl-2-propanone. These structures can be described as gauche (g; Figure 5A) or anti (a; Figure 5B) with respect to the torsional angle $\tau_1 = C_\varphi{-}C_1{-}C_2{-}C_3$. The relative energies of the two conformers are given in Table 6: the gauche structure was found to be 4.5 kJ mol^{-1} more stable than the anti configuration at the MP2/6-31G* level, and the MP2/6-311++G** single-point calculation indicates that g is more stable than a by 6.1 kJ mol^{-1}. The gauche structure is consistent with the three experimental moments of inertia, $\Delta I_{rms} = 9.9$ u Å,^{2} and the dipole moment projections (see Table 6), while the anti structure is inconsistent with the experimental data ($\Delta I_{rms} = 44.3$ u Å^2).

The torsional angle τ_1 changed from 60° to 81° upon optimization of the gauche structure. The methyl rotor makes

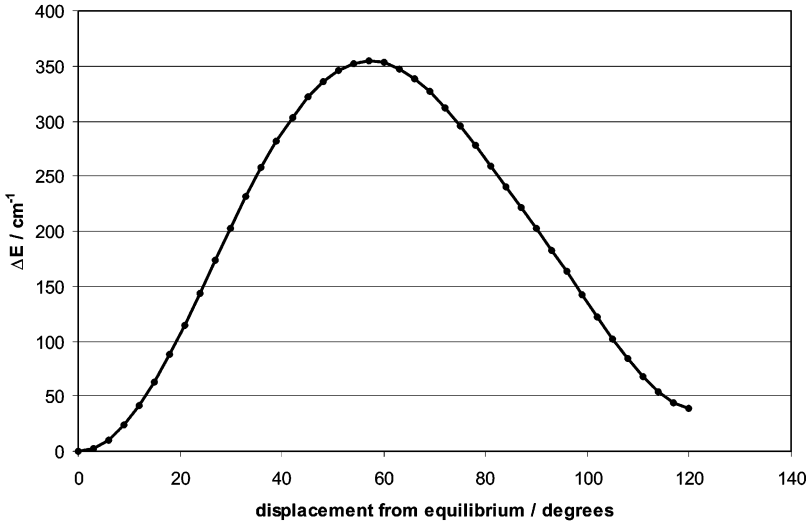

Figure 6. Relative energy of the gauche conformer of 1-phenyl-2-propanone as a function of the methyl internal rotation coordinate.

an angle of 80° with the *a*-inertial axis in the optimized structure; the rotor axis intersects both the *b*- and *c*-inertial axes with a 46° angle. The corresponding rotor-axis angles for the anti structure are $\theta_a = 22°$, $\theta_b = 68°$, and $\theta_c = 90°$. The rotor angles confirm the identity of the gauche conformational form of 1-phenyl-2-propanone.

Takahashi et al. previously identified the gauche conformer of 1-phenyl-2-propanone to be the most stable structure.[6] The authors attribute the stability of the gauche structure to weak CH$-\pi$ hydrogen bonds from one methyl hydrogen to the aromatic π electrons as well as from the ortho hydrogen to the carbonyl π electrons. These weak hydrogen bonds were inferred from short intramolecular distances (CH$-C_{\varphi}$ = 2.925 Å, C_{ortho}H$-O$ = 2.796 Å, and C_{ortho}H$-C_2$ = 2.929 Å).

The CH$-\pi$ hydrogen bond is broken and re-formed during internal rotation of the methyl group, so the barrier to internal rotation provides a measure of the strength of the hydrogen bond. We calculated the barrier to internal rotation of the methyl group by performing partial optimizations of the gauche conformer of 1-phenyl-2-propanone at the MP2/6-31G* level. The $C_1-C_2-C_3-$H torsional angle was fixed in 3° increments, while the rest of the structural coordinates were allowed to optimize. A plot of the relative energy as a function of torsional angle in the range 0−120° is shown in Figure 6. The barrier to internal rotation of the methyl group was found to be 355 cm^{-1} (4.2 kJ mol^{-1}), about 50% larger than the spectroscopic value for the barrier V_3. Nonetheless, the 4.2 kJ mol^{-1} barrier is comparable to the energy difference between the gauche and anti conformers (4.5 kJ mol^{-1} at this level of theory), strengthening the suggestion that the CH$-\pi$ hydrogen-bonding interaction is responsible for stabilizing the gauche conformer over the anti configuration.

Conclusions

Rotational spectra have been recorded for one conformational isomer of 1-phenyl-2-propanol, methamphetamine, and 1-phenyl-2-propanone. Optimized ab initio models identify these as the lowest energy conformations for each species. The optimized structures also reveal weak OH$-\pi$, NH$-\pi$, and CH$-\pi$ intramolecular hydrogen-bonding interactions that stabilize the lowest energy structures. The strength of this hydrogen-bonding interaction was quantified for 1-phenyl-2-propanone by fitting the experimental E-state transition frequencies to a V_3 internal rotation barrier (238 cm^{-1}) and by a series of ab initio partial optimizations along the internal rotation pathway (V_3 = 355 cm^{-1}).

Acknowledgment. This work was supported in part by a grant from the U.S. National Science Foundation (CHE-0240168). We thank Dr. Jeff Rowe (La Trobe University, Australia) for helpful discussions regarding the synthesis. Acknowledgment is also made to the Ohio Supercomputer Center for providing a grant of computer resources.

Supporting Information Available: Experimental frequencies and assignments of the rotational transitions for 1-phenyl-2-propanone, methamphetamine, and the A- and E-states of 1-phenyl-2-propanone. This material is available free of charge via the Internet at http://pubs.acs.org.

References and Notes

(1) Zigmond, M. J. *Fundamental Neuroscience*; Academic Press: San Diego, 1999.

(2) Brauer, L. H.; Goudie, A. J.; de Wit, H. *Psychopharmacology* **1997**, *130*, 2.

(3) Cho, W.; Taylor, L. P.; Akil, H. *Mol. Pharmacol.* **1996**, *50*, 1338.

(4) Sull, T. J.; Chass, G. A.; Varro, A.; Papp, J. G. *THEOCHEM* **2003**, *623*, 51.

(5) Takahashi, O.; Saito, K.; Kohno, Y.; Suezawa, H.; Ishihara, S.; Nishio, M. *Eur. J. Org. Chem.* **2004**, 2398.

(6) Takahashi, O.; Kohno, Y.; Saito, K.; Nishio, M. *Chem.—Eur. J.* **2003**, *9*, 756.

(7) Fraser, G. T.; Suenram, R. D.; Lugez, C. L. *J. Phys. Chem. A* **2001**, *105*, 9859.

(8) Fisher, J. M.; Xu, L. H.; Suenram, R. D.; Pate, B. H.; Douglass, K. O. *J. Mol. Struct.*, in press.

(9) Lavrich, R. J.; Plusquellic, D. F.; Suenram, R. D.; Fraser, G. T.; Hight Walker, A. R.; Tubergen, M. J. *J. Chem. Phys.* **2003**, *118*, 1253.

(10) Kawashima, Y.; Usami, T.; Ohashi, N.; Suenram, R. D.; Hougen, J. T.; Hirota, E. *Acc. Chem. Res.* **2006**, *39*, 216.

(11) Suenram, R. D.; Grabow, J.-U.; Zuban, A.; Leonov, I. *Rev. Sci. Instrum.* **1999**, *70*, 2127.

(12) Certain commercial products are identified in this paper to specify adequately the experimental or theoretical procedures. In no case does such identification imply recommendation or endorsement by the National Institute of Standards and Technology, nor does it imply that the products are necessarily the best available for the purpose.

(13) Suenram, R. D.; Lovas, F. J.; Plusquellic, D. F.; Lesarri, A.; Kawashima, Y.; Jensen, J. O.; Samuels, A. C. *J. Mol. Spectrosc.* **2002**, *211*, 110.

(14) Taylor, B. N.; Kuyatt, C. E. NIST Technical Note 1297; U.S. Government Printing Office: Washington, DC, 1994.

(15) Frisch, M. J.; Trucks, G. W.; Schlegel, H. B.; Scuseria, G. E.; Robb, M. A.; Cheeseman, J. R.; Montgomery, J. A., Jr.; Vreven, T.; Kudin, K. N.; Burant, J. C.; Millam, J. M.; Iyengar, S. S.; Tomasi, J.; Barone, V.;

Mennucci, B.; Cossi, M.; Scalmani, G.; Rega, N.; Petersson, G. A.; Nakatsuji, H.; Hada, M.; Ehara, M.; Toyota, K.; Fukuda, R.; Hasegawa, J.; Ishida, M.; Nakajima, T.; Honda, Y.; Kitao, O.; Nakai, H.; Klene, M.; Li, X.; Knox, J. E.; Hratchian, H. P.; Cross, J. B.; Adamo, C.; Jaramillo, J.; Gomperts, R.; Stratmann, R. E.; Yazyev, O.; Austin, A. J.; Cammi, R.; Pomelli, C.; Ochterski, J. W.; Ayala, P. Y.; Morokuma, K.; Voth, G. A.; Salvador, P.; Dannenberg, J. J.; Zakrzewski, V. G.; Dapprich, S.; Daniels, A. D.; Strain, M. C.; Farkas, O.; Malick, D. K.; Rabuck, A. D.; Raghavachari, K.; Foresman, J. B.; Ortiz, J. V.; Cui, Q.; Baboul, A. G.; Clifford, S.; Cioslowski, J.; Stefanov, B. B.; Liu, G.; Liashenko, A.; Piskorz, P.; Komaromi, I.; Martin, R. L.; Fox, D. J.; Keith, T.; Al-Laham, M. A.; Peng, C. Y.; Nanayakkara, A.; Challacombe, M.; Gill, P. M. W.; Johnson, B.; Chen, W.; Wong, M. W.; Gonzalez, C.; Pople, J. A. *Gaussian03*, revision C.02; Gaussian, Inc.: Wallingford, CT, 2004.

(16) Watson, J. K. G. *J. Chem. Phys.* **1967**, *46*, 1935.

(17) Pickett, H. M. *J. Mol. Spectrosc.* **1991**, *148*, 371.

(18) The CALPGM suite of programs can be found at the following JPL Web address: http://spec.jpl.nasa.gov.

(19) Jeffrey, G. A.; Saenger, W. *Hydrogen Bonding in Biological Structures*; Springer: Berlin, 1991.

(20) The JB95 spectral fitting program can be downloaded from the following NIST Web address: http://physics.nist.gov/Divisions/Div844/facilities/uvs/jb95userguide.htm.

(21) Lavrich, R. J.; Hight Walker, A. R.; Plusquellic, D. F.; Kliener, I.; Suenram, R. D.; Hougen, J. T.; Fraser, G. T. *J. Chem. Phys.* **2003**, *119*, 5497.

(22) Lavrich, R. J.; Plusquellic, D. F.; Suenram, R. D.; Fraser, G. T.; Hight Walker, A. R.; Tubergen, M. J. *J. Chem. Phys.*, manuscript in preparation.